

Dyes/Pigments

Color Tuning of the Aggregation-Induced Emission of Maleimide Dyes by Molecular Design and Morphology Control

Hiroaki Imoto,^[a] Kohei Kizaki,^[a] Seiji Watase,^[b] Kimihiro Matsukawa,^[b] and Kensuke Naka*^[a]

Abstract: Aggregation-induced emission (AIE)-active maleimide dyes, namely, 2-*p*-toluidino-*N*-*p*-tolylmaleimide, 3-phenyl-2-toluidino-*N*-*p*-tolylmaleimide, 2-*p*-thiocresyl-3-*p*-toluidino-*N*-*p*-tolylmaleimide, and 2,3-dithiocresyl-*N*-arylmaleimides, were synthesized by facile synthetic procedures. The dyes show intense emission in the solid state, and emission colors were controlled from green ($\lambda_{\text{max}}=527$ nm) to orange ($\lambda_{\text{max}}=609$ nm) by varying the substituents at the 2- and 3-positions of the maleimide and the packing structures in the solid state. 2,3-Disubstituted maleimide dyes effectively un-

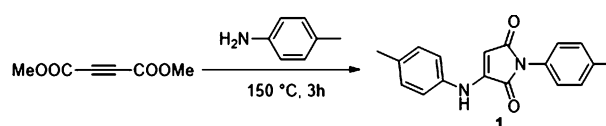
derwent redshifts of their emission wavelength. Furthermore, some of the dyes exhibited mechanochromism and polymorphism, and their emission properties were dramatically dependent on the morphology of the solid samples. The mechanisms of the emission behaviors were investigated by X-ray diffraction. The substituent of the nitrogen atom of the maleimide ring affected the intermolecular interactions and short contacts, which were observed by single crystal X-ray crystallography, to result in completely different emission properties.

Introduction

Solid-state emission is a key property for developing luminescent materials.^[1] Much research has been carried out to achieve intense emission in the solid state.^[2] Aggregation-induced emission (AIE) is very effective strategy to accomplish this goal.^[3] After the landmark research of Tang and co-workers in 2001,^[4] various kinds of AIE-active dyes have been reported, such as tetraphenylsilole,^[4,5] tetraphenylethylene,^[6] and so on.^[7] The basic strategies for the molecular design of solid-state emission are restriction of non-emissive deactivation due to molecular motions and suppression of concentration self-quenching. For example, excitons of tetraphenylsilole are deactivated by rotation of the phenyl groups and twisting of the C=C bond in a good solvent, but these molecular motions are frozen in the solid state.^[8] In addition, steric hindrance of propeller-shaped molecular structures inhibits concentration self-quenching.

On the other hand, most such dyes require complicated synthetic routes starting from commercially available compounds.^[9] Facile synthetic methods for AIE dyes are still desired not only in academic research, but also for industrial applica-

tions. The maleimide skeleton has attracted much attention for luminescent materials because of its simple and versatile molecular structure.^[10,11] Several works reported 2,3-diaryl maleimides showing various emission colors in solution^[10] and luminescent polymers from 2,3-disubstituted maleimide monomers.^[11] However, there is no research on AIE of maleimide dyes. Recently, we have developed AIE-active amino maleimide derivatives^[12,13] that can be synthesized in a one-pot process (Scheme 1).^[13] Amino maleimide derivatives such as 2-*p*-toluidi-



Scheme 1. Synthesis of amino maleimide 1.^[13]

no-*N*-*p*-tolylmaleimide (1) exhibit green emission under UV irradiation in the solid state, but no emission is observed in good solvents. Free rotation of the secondary aryl amine deactivates the excitons by a non-emissive pathway in good solvents. The molecular motion is restricted in the solid state, and X-ray crystallography revealed an edge-to-face packing structure that prevents self-quenching. These dyes are potential candidates for solid-state emission materials because of their availability and designability. Color tuning of AIE-active maleimide dyes is required to expand their versatility for applications.

Our previous theoretical study on 2-aryl amino maleimides indicated that a luminescent center is localized at the five-membered maleimide ring and the secondary aryl amine.^[13] Hence, the 2- and 3-positions of the maleimide rings are thought to be dominant for the emission color of the malei-

[a] Dr. H. Imoto, K. Kizaki, Prof. K. Naka
Faculty of Molecular Chemistry and Engineering
Graduate School of Science and Technology
Kyoto Institute of Technology
Goshokaido-cho, Matsugasaki, Sakyo-ku, Kyoto 606-8585 (Japan)
E-mail: kenaka@kit.ac.jp

[b] Dr. S. Watase, Dr. K. Matsukawa
Osaka Municipal Technical Research Institute
1-6-50 Morinomiya, Joto-ku, Osaka 536-8553 (Japan)

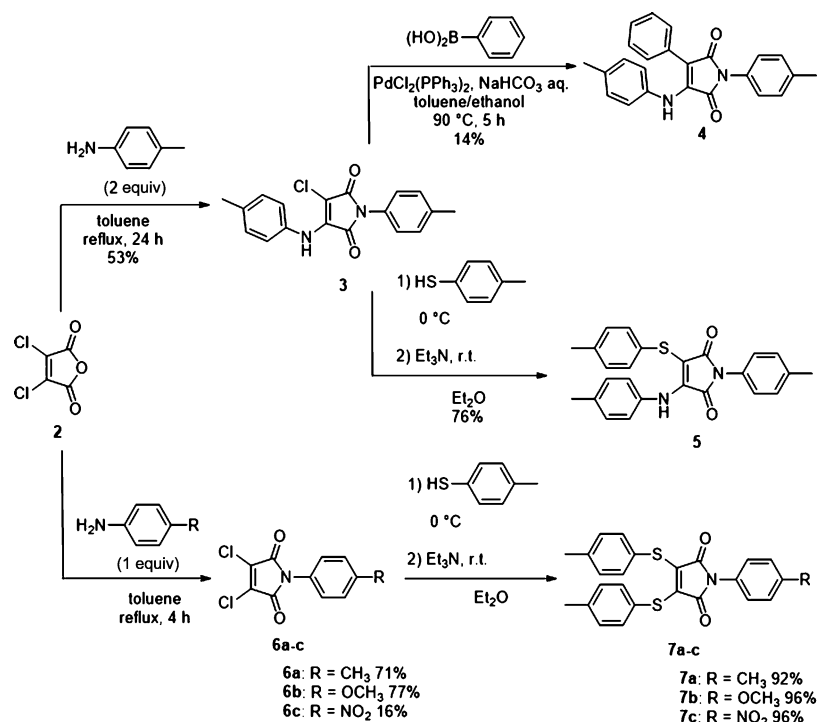
Supporting information for this article is available on the WWW under <http://dx.doi.org/10.1002/chem.201501519>.

mid dyes. Herein, 2,3-disubstituted amino maleimides and their thioether analogues were investigated to achieve longer emission wavelengths than those of the 2-aryl amino maleimides we reported.^[12] These designed maleimide derivatives seemed to show AIE activity because free rotation around the secondary amine and/or the thiol could deactivate the excitons effectively in solution. We also found that some of the present maleimide dyes displayed unique emission behaviors derived from polymorphism^[14,15] and mechanochromism.^[14,16] This is the first study on color tuning of AIE-active maleimide dyes on the basis of molecular design and morphology control.

Results and Discussion

Synthesis of maleimide dyes

We synthesized 3-phenyl-2-toluidino-*N-p*-tolylmaleimide (**4**), 2-*p*-thiocresyl-3-*p*-toluidino-*N-p*-tolylmaleimide (**5**), and 2,3-dithiocresyl-*N*-arylmaleimides **7a–7c** by facile synthetic procedures (Scheme 2).



Scheme 2. Synthesis of maleimide derivatives from **2**.

One-pot transformation of 2,3-dichloromaleic anhydride (**2**) into monosubstituted imide 3-*p*-toluidino-2-chloro-*N-p*-tolylmaleimide (**3**) proceeded with two equivalents of *p*-toluidine in toluene under reflux for 24 h. Subsequently, Pd-catalyzed Suzuki–Miyaura coupling reaction^[17] of **3** and phenylboronic acid at 90 °C for 5 h led to **4** after purification by silica-gel chromatography and recrystallization from dichloromethane and methanol.^[18] Nucleophilic substitution of **3** with *p*-thiocresyl was performed in diethyl ether at 0 °C, and subsequent addi-

tion of triethylamine lead to a yellowish precipitate of **5** after stirring at room temperature for 16 h.^[19]

Compound **2** was converted to 2,3-dichloro-*N*-arylmaleimides **6a–6c** with one equivalent of *p*-substituted aniline in toluene under reflux for 4 h.^[20] The same synthetic procedure as that of **5** resulted in **7a–7c**. It is noteworthy that purification only required washing with methanol, except for **4**. The chemical structures of the newly synthesized compounds were confirmed by ¹H and ¹³C NMR spectroscopy and high-resolution mass spectrometry.^[21]

Optical properties

The optical properties of the maleimide dyes are summarized in Table 1. The absorption spectra were measured in solution ($c = 1.0 \times 10^{-4}$ M in dichloromethane). The absorption maxima were redshifted by introduction of substituents in the 2- and 3-positions in comparison to **1** ($\lambda_{\text{max}} = 386$ nm). The phenyl group of **4** and the thiocresyl group of **5** caused redshifts of the absorption maxima relative to **1** by 14 and 21 nm, respectively,

probably because the electron-donating thiocresyl and phenyl groups raised the HOMO levels and thus narrowed the HOMO–LUMO gaps. The thiocresyl group was more effective in narrowing the HOMO–LUMO gap than the phenyl group. Thus, longer wavelengths of the absorption maxima of **7a–7c** were attained in comparison to **5** by changing the substituents from tolyldyl to thiocresyl. Electron-donating or electron-rich substituents at the 2- and 3-positions are reported to cause redshifts of the absorption maxima.^[10] On the other hand, the wavelengths of the absorption maxima of **7a–7c** were approximately same because the *N*-substituents^[22] of **7a–7c** had little effect on HOMOs and LUMOs (Supporting Information, Figure S18).

All the maleimide derivatives studied here showed no emission in good solvents such as dichloromethane, chloroform, and THF because of free rotation about flexible amine and/or thiol bonds in the luminophores in solutions. However, they showed luminescence in the solid state due to restriction of rotation, which suggests that they have AIE activity. The solid samples for measurement of photoluminescence (PL) spectra were prepared by recrystallization. In the case of **7a**, three types of crystals were obtained (**7a₁–7a₃**). The emission wavelengths of the 2,3-disubstituted maleimide dyes ($\lambda_{\text{max}} = 553–609$ nm) were redshifted from that of

Compound	$\lambda_{\text{abs,sol}}^{\text{[a]}}$	Solid state			
		Color	Shape	$\lambda_{\text{PL,solid}}^{\text{[b]}}$	$\Phi_{\text{PL,solid}}^{\text{[c]}}$
1	386 ^[d]	yellow	precipitate	527 ^[d]	0.07 ^[d]
4	400	yellow	cubic	553	0.03
5	407	orange	fiber	578	0.02
		orange	cubic (7a ₁)	591	< 0.01
7a	430	yellow	needle (7a ₂)	555	< 0.01
		orange	needle (7a ₃)	606	0.14
7b	430	orange	cubic	609	< 0.01
7c	435	yellow	needle	562	0.03

[a] Absorption maxima in dichloromethane ($c = 1.0 \times 10^{-4}$ M). [b] PL maximum wavelength in the solid state. [c] Absolute quantum yield in the solid state. [d] Ref. [13].

1 ($\lambda_{\text{max}} = 527$ nm). Generally, as the substituents of the 2- and 3-positions became more electron rich, the emission wavelength became longer; this tendency is in good accordance with their absorption wavelengths. The emission wavelengths of **4** and **5** were shifted from that of **1** ($\lambda_{\text{max}} = 527$ nm) to 553 and 578 nm, respectively. As described previously, the emission colors are controlled by the substituents on the 2- and 3-positions.^[10,11] The emission properties of **7a**–**7c** were quite different due to the effect of the *N*-substituents, despite the similar absorption spectra in solution. In addition, we found that **4** showed mechanochromism; emission color reversibly changed between green and yellow on mechanical stimulus and treatment with dichloromethane. Emission properties were affected by not only chemical structures, but also by packing structures.

Mechanochromism

The PL spectra and emission behavior of **4** are shown in Figure 1. The emission color of **4** after recrystallization from dichloromethane and methanol (**4**_{cryst}) was different from that of

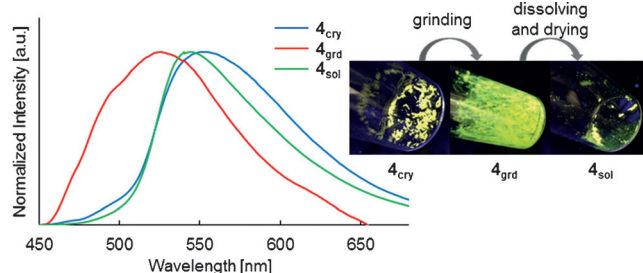


Figure 1. PL spectra (left) and photographs (right) of solid **4**_{cryst}, **4**_{grd}, and **4**_{sol} under UV irradiation at 365 nm.

the sample ground in a mortar (**4**_{grd}). The yellow emission (553 nm, $\Phi_{\text{PL}} = 0.03$) of **4**_{cryst} changed to green emission (525 nm, $\Phi_{\text{PL}} = 0.03$) of **4**_{grd}. Solid **4**_{grd} was dissolved in dichloromethane, and subsequently the solvent was removed to obtain a dried residue (**4**_{sol}). The emission maximum wavelength of **4**_{sol} was 545 nm ($\Phi_{\text{PL}} = 0.04$), similar to that of **4**_{cryst}.

The emission color of **4** was reversibly changed by external mechanical stimulus.

To explore the difference in morphology between these states, XRD analysis was carried out (Supporting Information, Figure S17). The XRD pattern of **4**_{cryst} showed defined diffraction peaks, whereas that of **4**_{grd} showed only a halo peak, which reveals amorphous character of **4**_{grd}. The defined peaks were recovered in **4**_{sol}, though the diffraction pattern was different from that of **4**_{cryst}. Crystalline-to-amorphous and amorphous-to-crystalline transitions caused blue- and redshift of the PL spectra, respectively. Such a color change due to the phase transition suggests that the maleimide ring as a luminescent center must be strongly affected by close contacts to adjacent molecules. Since conformational flexibility of the thiol can induce unspecified contacts among molecules on external stimulus, various intermolecular interactions formed as local structure may lead to mechanochromism. In addition, mechanochromism was observed only in **4**, whereas the emission colors of other dyes were not changed by grinding. Therefore, the rigid and bulky phenyl group at the 3-position regulated formation of a robust hydrogen-bond network, as was observed in **1**.^[12] As a result, mechanical stimulus can cause crystalline-to-amorphous transition. The detailed mechanism of the mechanochromism is under investigation.

Polymorphism

Polymorphism of **7a** was examined. Solid **7a** was obtained as an orange precipitate after the reaction, and subsequent recrystallization from dichloromethane and methanol gave mixture of cubic orange crystals of **7a**₁ and needlelike yellow crystals of **7a**₂. Besides, needlelike orange crystals of **7a**₃ were obtained by recrystallization from dichloromethane and methanol under relatively dilute conditions. We confirmed that all the solid samples **7a**₁–**7a**₃ were composed of the same compound by ¹H and ¹³C NMR spectroscopy. For further verification, **7a**₂ was dissolved in dichloromethane, and recrystallization was performed by adding methanol under dilute conditions. Eventually, needlelike orange crystals of **7a**₃ were isolated.

Each crystal form of **7a** exhibited different emission wavelengths and quantum yields. Thus, **7a**₃ exhibited more intensive emission at longer wavelength ($\lambda_{\text{max}} = 606$ nm, $\Phi_{\text{PL}} = 0.14$) than **7a**₁ ($\lambda_{\text{max}} = 591$ nm, $\Phi_{\text{PL}} < 0.01$) and **7a**₂ ($\lambda_{\text{max}} = 555$ nm, $\Phi_{\text{PL}} > 0.01$). Therefore, it is thought that the crystal packing strongly affected their emission properties. We carried out XRD analysis to compare the morphologies of **7a**₁–**7a**₃. The diffraction patterns of **7a**₁–**7a**₃ clearly differed from each other (Figure 2, left). This indicates that **7a** can form three types of polymorph that have different emission behaviors in the solid state (Figure 2, right). Flexibility of the two thioether bonds probably allowed for various types of induced packing.

Crystallographic study

For further understanding of the effects of packing structure, we performed single-crystal XRD of **7b** and **7c** (Figure 3).^[23] They showed different solid-state emission properties, al-

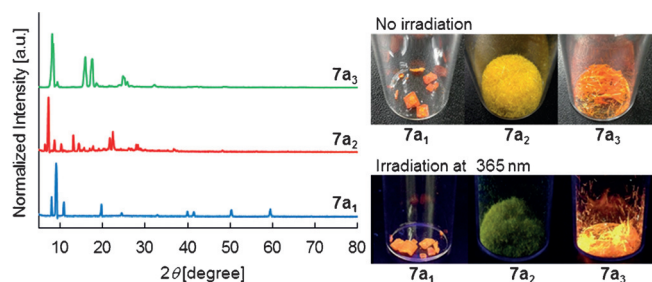


Figure 2. XRD patterns (left) and photographs (right) of **7a**₁–**7a**₃ under UV irradiation at 365 nm.

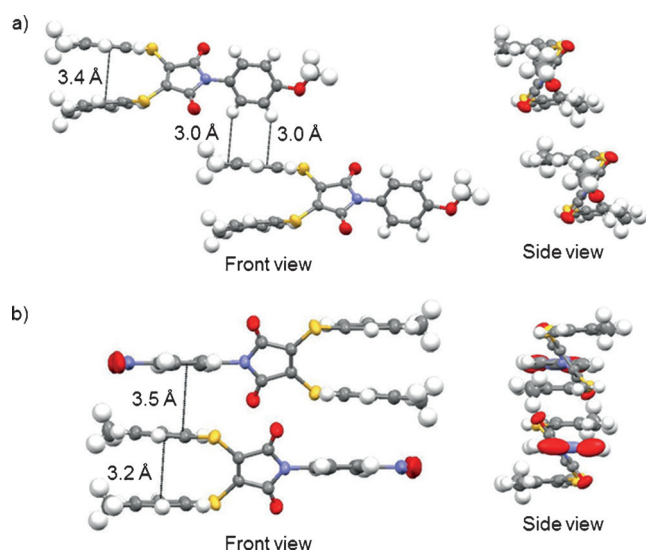


Figure 3. Molecular packing in the crystal structures of a) **7b** and b) **7c** with ellipsoids at 50% probability.

though they had approximately the same UV/Vis absorption maxima in solution (Table 1). Suitable single crystals for XRD analysis were prepared by slow mixing of methanol with dichloromethane solutions, and **7b** and **7c** crystallized in the triclinic $P\bar{1}$ and monoclinic $P2_1/c$ space groups, respectively. Both compounds showed intramolecular π – π stacking of the *S*-substituted benzene rings,^[24] and the average distances between the two benzene rings were approximately 3.4 and 3.2 Å, respectively. DFT calculations (Supporting Information, Figure S18) revealed that the LUMOs of **7b** and **7c** are located mainly at the five-membered maleimide rings, which are aligned in a nonparallel manner that restricts concentration self-quenching in the crystals. In contrast to the similar intramolecular interactions, the intermolecular interactions of **7b** and **7c** were substantially different. In the crystal packing of **7b**, intermolecular edge-to-face CH– π interaction of the *S*-substituted benzene rings was observed, and the average distance from the protons to the mean plane of the *S*-substituted benzene rings is approximately 3.0 Å. In the crystalline packing of **7c**, on the other hand, the *S*-substituted benzene rings interact with the *N*-substituted benzene rings, and the average distance between the two benzene rings is approximately 3.5 Å.

The steric hindrance of the methoxyl group of **7b** possibly inhibits the intermolecular face-to-face π – π stacking. The molecular packing seemed to be a key factor in the emission properties of **7b** and **7c**, which were caused by the different intermolecular interactions. The above-described formation of intermolecular π – π stacking and CH– π interactions is not sufficient to explain the difference in their emission properties.

We focused on the local surroundings of a maleimide lumiphore in the crystals to explain the emission behaviors of **7b** and **7c** (Figure 4). The maleimide ring of **7b** interacts with

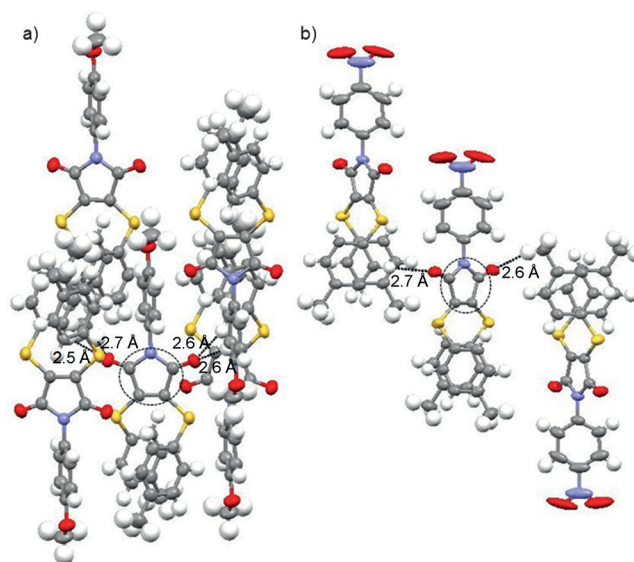


Figure 4. Surroundings of the luminescent centers (dashed lines) of a) **7b** and b) **7c** in the crystalline state.

four neighboring molecules in the crystal through hydrogen bonds (2.5–2.7 Å) between the electron-rich C=O and electron poor C–H bonds, whereas that of **7c** interacts with two molecules (2.6–2.7 Å). Such short contacts can lower the electron density of the maleimide ring, and may reduce the HOMO–LUMO gap, causing the redshift of the absorption and PL spectra. In fact, the absorption edges of the diffuse-reflection spectra of **7b** and **7c** were observed around 590 and 560 nm, respectively (Supporting Information, Figure S19), contrary to the trend of the wavelengths of their absorption maxima in solutions. In the solid-state, the peak maximum of **7b** was also observed at longer wavelength (609 nm) than that of **7c** (562 nm). Thus, it suggests that the number of short contacts in the local area near the luminophore is strongly related to the emission properties.

Conclusion

We have described methodologies for color tuning of AIE-active maleimide dyes by molecular design and morphology control. The luminophore is located at the five-membered maleimide ring, and its electronic state can be controlled by the substituents in the 2- and 3-positions. Hence, the introduction of thiocresyl, toluidyl, and phenyl groups in the maleimides

drastically changed their emission colors. In addition, packing structures strongly affected the emission properties. We found that **4** exhibits mechanochromism; grinding the crystals caused a blueshift, and treatment with dichloromethane led to recovery of the original emission. Solid **7a** showed three types of polymorphism, and the emission properties depended on the crystal packing. The packing structures in the solid state were varied by means of the *N*-substituted benzene ring to give completely different emission properties despite the similar absorption spectra in solution. Different modes of intermolecular interactions were observed in **7b** and **7c**. The local surroundings of the maleimide ring probably caused their different emission behaviors, though prediction of packing structures is difficult.

This study suggests that AIE-active maleimides are promising candidates as multicolor luminescent dyes, stimuli-responsive materials, and so on. Their simple molecular structures and facile synthetic procedures are attractive for practical applications. Expansion to full-color emission, other functions of maleimide dyes, and detailed mechanisms of their unique properties are under research.

Experimental Section

Materials

Toluene, methanol, triethylamine, ethanol, diethyl ether, ethyl acetate, hexane, and dichloromethane were purchased from Nacal Tesque, Inc. Dichloro maleic anhydride (**2**), *p*-toluidine, *p*-anisidine, *p*-nitroaniline, *p*-toluenethiol, [PdCl₂(PPh₃)₂], distilled water, silica gel (Wakogel C-200), and magnesium sulfate anhydrous (MgSO₄) were purchased from Wako Pure Chemical Industry, Ltd. Phenylboronic acid was purchased from Tokyo Chemical Industry Co., Ltd. All commercially available chemicals were used without any purification. 2-*p*-Toluidino-*N*-*p*-tolylmaleimide (**1**) was prepared by following our previous paper.^[13]

Measurements

¹H (400 MHz) and ¹³C (100 MHz) NMR spectra were recorded on a Bruker DPX-400 spectrometer in CDCl₃ and [D₆]DMSO with Me₄Si as internal standard. High-resolution mass spectra were obtained on a JEOL JMS-SX102A spectrometer. UV/Vis spectra were recorded on a Jasco spectrophotometer V-670 KKN. Emission spectra were obtained on an JASCO fluorescence spectrophotometer FP-8500. XRD data were recorded on a Smart Lab (Rigaku) with Cu_{Kα} radiation (λ = 1.5406 Å) in θ/2θ mode at room temperature. The 2θ scans were collected at 0.01° intervals, and the scan speed was 2° min⁻¹ in 2θ.

XRD of single-crystalline products

Single crystals were mounted on glass fibers with epoxy resin. Intensity data were collected at room temperature on a Rigaku RAXIS RAPID II imaging-plate area detector with graphite-monochromated Mo_{Kα} radiation. The crystal-to-detector distance was 127.40 mm. Readout was performed in the 0.100 mm pixel mode. The data were collected at room temperature to a maximum 2θ value of 55.0°. Data were processed by the PROCESS-AUTO^[25] program package. An empirical or numerical absorption correction^[26] was applied. The data were corrected for Lorentzian and polariza-

tion effects. A correction for secondary extinction^[27] was applied. The structures were solved by heavy-atom Patterson methods^[28] and expanded by using Fourier techniques.^[29] Some non-hydrogen atoms were refined anisotropically, and the rest were refined isotropically. Hydrogen atoms were refined by using the riding model. The final cycle of full-matrix least-squares refinement on *F*² was based on observed reflections and variable parameters. In the case of the crystalline product recrystallized from acetone, the final cycle of full-matrix least-squares refinement on *F* was based on observed reflections and variable parameters. All calculations were performed with the CrystalStructure^[30,31] crystallographic software package. Crystal data and further information on XRD data collection are summarized in Tables S1 and S2 of the Supporting Information.

Synthesis

3-*p*-Toluidino-2-chloro-*N*-*p*-tolylmaleimide (3**):** The synthetic procedure followed the literature.^[20] A toluene solution (20 mL) of **2** (0.784 g, 4.69 mmol) and *p*-toluidine (1.00 g, 9.34 mmol) was heated to reflux for 24 h. After the reaction, the solvent was removed in vacuo, and the residue was washed with methanol to give **3** as yellow solid 0.812 g (2.49 mmol, 53%). ¹H NMR ([D₆]DMSO, 400 MHz): δ = 9.88 (s, 1H), 7.28–7.11 (m, 8H), 2.35 (s, 3H), 2.30 ppm (s, 3H). The solubility was too low to measure the ¹³C NMR spectrum.

3-Phenyl-2-toluidino-*N*-*p*-tolylmaleimide (4**):** The synthetic procedure followed the literature.^[19] A saturated aqueous solution (6.5 mL) of NaHCO₃ was added to a solution of **3** (0.479 g, 1.47 mmol), phenylboronic acid (0.225 g, 1.85 mmol), and [PdCl₂(PPh₃)₂] (86.4 mg, 0.123 mmol) in toluene (15 mL) and ethanol (10 mL). The reaction mixture was heated at 90 °C under N₂ atmosphere for 5 h. After cooling to room temperature, distilled water (30 mL) was added, and the organic layer was extracted with EtOAc (50 mL × 2). The combined organic layers were washed with brine (50 mL × 3), and dried over MgSO₄. After filtration, the solvents were removed in vacuo. The residue was subjected to short-column chromatography on silica gel with hexane/EtOAc = 20/1 (*R_f* = 0.9) as eluent and recrystallization from dichloromethane and methanol to give **4** as a yellow solid (76 mg, 0.206 mmol, 14%). ¹H NMR (CDCl₃, 400 MHz): δ = 7.37–7.27 (m, 5H), 7.15–7.07 (m, 5H), 6.85 (d, *J* = 8.4 Hz, 2H), 6.58 (d, *J* = 8.4 Hz, 2H), 2.40 (s, 3H), 2.23 ppm (s, 3H). The solubility was too low to measure the ¹³C NMR spectrum. HRMS (FAB) calcd for C₂₄H₂₀N₂O₂ [M]⁺: 368.1525; found: 368.1519.

2-*p*-Thiocresyl-3-*p*-toluidino-*N*-*p*-tolylmaleimide (5**):** An Et₂O solution (10 mL) of **3** (99.7 mg, 0.305 mmol) and *p*-toluenethiol (44.8 mg, 0.361 mmol) was stirred at 0 °C for 5 min, and subsequently triethylamine (3.85 g, 38.0 mmol) was added. After stirring at room temperature for 16 h, the solvent was removed in vacuo, and the residue was washed with methanol to give **5** as yellow solid (96 mg, 0.232 mmol, 76%). ¹H NMR (CDCl₃, 400 MHz): δ = 7.41–6.88 (m, 13H), 2.38 (s, 3H), 2.35 (s, 3H), 2.26 ppm (s, 3H). The solubility was too low to measure the ¹³C NMR spectrum. HRMS (FAB) calcd for C₂₅H₂₂N₂O₂S [M]⁺: 414.1402; found: 414.1406.

2,3-Dichlo-*N*-*p*-tolylmaleimide (6a**):** The synthetic procedure followed the literature.^[20] A toluene solution (15 mL) of **2** (2.00 g, 12.1 mmol) and *p*-toluidine (1.29 g, 12.0 mmol) was heated to reflux for 4 h. After the reaction, the solvent was removed in vacuo, and the residue was washed with methanol to give **6a** as a colorless solid 2.18 g (8.52 mmol, 71%). ¹H NMR (CDCl₃, 400 MHz): δ = 7.27 (d, *J* = 8.8 Hz, 2H), 7.19 (d, *J* = 8.4 Hz, 2H),

2.38 ppm (s, 3H); ^{13}C NMR (CDCl_3 , 100 MHz): $\delta = 162.1, 138.9, 133.5, 130.0, 127.9, 126.0, 21.2$ ppm.

2,3-Dichloro-*N*-*p*-anisoylmaleimide (6b): A toluene solution (20 mL) of **2** (1.00 g, 6.02 mmol) and *p*-anisidine (0.742 g, 6.03 mmol) was heated to reflux for 4 h. After the reaction, the solvent was removed in vacuo, and the residue was washed with methanol to give **6b** as a colorless solid (1.26 g, 4.64 mmol, 77%). ^1H NMR (CDCl_3 , 400 MHz): $\delta = 7.23$ (d, $J = 8.8$ Hz, 2H), 6.98 (d, $J = 8.8$ Hz, 2H), 3.84 ppm (s, 3H); ^{13}C NMR (CDCl_3 , 100 MHz): $\delta = 162.3, 159.7, 133.5, 127.6, 123.1, 114.7, 55.5$ ppm.

2,3-Dichloro-*N*-*p*-nitrophenylmaleimide (6c): A toluene solution (15 mL) of **2** (2.00 g, 12.0 mmol) and *p*-nitroaniline (1.66 g, 12.0 mmol) was heated to reflux for 4 h. After the reaction, the solvent was removed in vacuo, and the residue was washed with methanol to give **6c** as a colorless solid (0.55 g, 1.92 mmol, 16%). ^1H NMR (CDCl_3 , 400 MHz): $\delta = 8.36$ (d, $J = 9.2$ Hz, 2H), 7.67 ppm (d, $J = 9.2$ Hz, 2H); ^{13}C NMR (CDCl_3 , 100 MHz): $\delta = 161.2, 146.7, 136.2, 134.2, 125.7, 124.7$ ppm.

2,3-Dithiobis(*N*-*p*-tolylmaleimide (7a): An Et_2O solution (10 mL) of **6a** (0.300 g, 1.17 mmol) and *p*-toluenethiol (0.296 g, 2.39 mmol) was stirred at 0°C for 5 min, and subsequently triethylamine (0.247 g, 2.44 mmol) was added. After stirring at room temperature for 16 h, the solvent was removed in vacuo, and the residue was washed with methanol to give **7a** as a yellow solid (0.465 g, 1.08 mmol, 92%). ^1H NMR (CDCl_3 , 400 MHz): $\delta = 7.23$ (d, $J = 8.4$ Hz, 4H), 7.17 (s, 4H), 7.09 (d, $J = 8.0$ Hz, 4H), 2.33 ppm (s, 9H); ^{13}C NMR (CDCl_3 , 100 MHz): $\delta = 165.7, 139.0, 137.8, 136.1, 132.7, 129.9, 129.6, 128.8, 125.8, 125.5, 21.3, 21.1$ ppm; HRMS (FAB) calcd for $\text{C}_{25}\text{H}_{21}\text{NO}_2\text{S}_2$ $[M]^+$: 431.1014; found: 431.1007.

2,3-Dithiobis(*N*-*p*-anisoylmaleimide (7b): An Et_2O solution (10 mL) of **6b** (0.499 g, 1.83 mmol) and *p*-toluenethiol (0.474 g, 3.82 mmol) was stirred at 0°C for 5 min, and subsequently triethylamine (0.380 g, 3.76 mmol) was added. After stirring at room temperature for 16 h, the solvent was removed in vacuo, and the residue was washed with methanol to give **7b** as an orange solid (0.786 g (1.76 mmol, 96%). ^1H NMR (CDCl_3 , 400 MHz): $\delta = 7.24\text{--}7.18$ (m, 6H), 7.09 (d, $J = 8.0$ Hz, 4H), 6.89 (d, $J = 9.2$ Hz, 2H), 3.77 (s, 3H), 2.33 ppm (s, 6H); ^{13}C NMR (CDCl_3 , 100 MHz): $\delta = 165.8, 159.0, 139.0, 136.0, 132.7, 129.9, 127.4, 125.5, 124.1, 114.3, 55.5, 21.3$ ppm; HRMS (FAB) calcd for $\text{C}_{25}\text{H}_{21}\text{NO}_3\text{S}_2$ $[M]^+$: 447.0963; found: 447.0972.

2,3-Dithiobis(*N*-*p*-nitrophenylmaleimide (7c): An Et_2O solution (10 mL) of **6c** (99.5 mg, 0.347 mmol) and *p*-toluenethiol (88.7 mg, 0.714 mmol) was stirred at 0°C for 5 min, and subsequently triethylamine (90 mg, 0.089 mmol) was added. After stirring at room temperature for 16 h, the solvent was removed in vacuo, and the residue was washed with methanol to give **7c** as a yellow solid (154 mg (0.333 mmol, 96%). ^1H NMR (CDCl_3 , 400 MHz): $\delta = 8.23$ (d, $J = 8.8$ Hz, 2H), 7.62 (d, $J = 9.2$ Hz, 2H), 7.26 (d, $J = 7.2$ Hz, 4H), 7.12 (d, $J = 8.0$ Hz, 4H), 2.35 ppm (s, 6H); ^{13}C NMR (CDCl_3 , 100 MHz): $\delta = 164.6, 145.9, 139.5, 137.3, 136.5, 132.9, 130.0, 125.3, 124.9, 124.3, 21.3$ ppm; HRMS (FAB) calcd for $\text{C}_{24}\text{H}_{18}\text{N}_2\text{O}_4\text{S}_2$ $[M]^+$: 462.0708; found: 462.0716.

Keywords: aggregation · dyes/pigments · luminescence · mechanochromism · polymorphism

- [1] a) K.-T. Wong, Y.-Y. Chien, R.-T. Chen, C.-F. Wang, Y.-T. Lin, H.-H. Chiang, P.-Y. Hsieh, C.-C. Wu, C. H. Chou, Y. O. Su, G.-H. Lee, S.-M. Peng, *J. Am. Chem. Soc.* **2002**, *124*, 11576; b) Z. Xie, B. Yang, F. Li, G. Cheng, L. Liu, G. Yang, H. Xu, L. Ye, M. Hanif, S. Liu, D. Ma, Y. Ma, *J. Am. Chem. Soc.* **2005**, *127*, 14152; c) C.-H. Zhao, A. Wakamiya, Y. Inukai, S. Yamaguchi, *J. Am. Chem. Soc.* **2006**, *128*, 15934; d) A. Wakamiya, K. Mori, S. Yamaguchi,

- Angew. Chem. Int. Ed.* **2007**, *46*, 4273; *Angew. Chem.* **2007**, *119*, 4351; e) C.-H. Zhao, A. Wakamiya, S. Yamaguchi, *Macromolecules* **2007**, *40*, 3898; f) M. Shimizu, K. Mochida, T. Hiyaama, *Angew. Chem. Int. Ed.* **2008**, *47*, 9760; *Angew. Chem.* **2008**, *120*, 9906; g) W.-Y. Lai, R. Xia, Q.-Y. He, P. A. Levermore, W. Huang, D. D. C. Bradley, *Adv. Mater.* **2009**, *21*, 355.
- [2] Recent papers, see: a) R. Yoshii, A. Hirose, K. Tanaka, Y. Chujo, *J. Am. Chem. Soc.* **2014**, *136*, 18131; b) R. Yoshii, A. Hirose, K. Tanaka, Y. Chujo, *Chem. Eur. J.* **2014**, *20*, 8320; c) P. Galer, R. C. Korošec, M. Vidmar, B. Šket, *J. Am. Chem. Soc.* **2014**, *136*, 7383; d) M. V. Ramakrishnam Raju, H.-C. Lin, *Org. Lett.* **2014**, *16*, 5564; e) A. Goel, A. Sharma, M. Rawat, R. S. Anand, R. Kant, *J. Org. Chem.* **2014**, *79*, 10873; f) H. Braunschweig, S. Ghosh, J. O. C. Jimenez-Halla, J. H. Klein, C. Lambert, K. Radacki, A. Steffen, A. Vargas, J. Wahler, *Chem. Eur. J.* **2015**, *21*, 210.
- [3] Reviews, see: a) Y. Hong, J. W. Y. Lam, B. Z. Tang, *Chem. Commun.* **2009**, 4332; b) D. Ding, K. Li, B. Liu, B. Z. Tang, *Acc. Chem. Res.* **2013**, *46*, 2441; c) R. Hu, N. L. C. Leung, B. Z. Tang, *Chem. Soc. Rev.* **2014**, *43*, 4494; d) J. Mei, Y. Hong, J. W. Y. Lam, A. Qin, Y. Tang, B. Z. Tang, *Adv. Mater.* **2014**, *26*, 5429.
- [4] J. Luo, Z. Xie, J. W. Y. Lam, L. Cheng, H. Chen, C. Qiu, H. S. Kwok, X. Zhan, Y. Liu, D. Zhu, B. Z. Tang, *Chem. Commun.* **2001**, 1740.
- [5] Z. Li, Y. W. Dong, J. W. Y. Lam, J. Sun, A. Qin, M. Häußler, Y. P. Dong, H. H. Y. Sung, I. D. Williams, H. S. Kwok, B. Z. Tang, *Adv. Funct. Mater.* **2009**, *19*, 905.
- [6] W. Z. Yuan, S. Chen, J. W. Y. Lam, C. Deng, P. Lu, H. H.-Y. Sung, I. D. Williams, H. S. Kwok, Y. Zhang, B. Z. Tang, *Chem. Commun.* **2011**, 47, 11216; Y. Liu, S. Chen, J. W. Y. Lam, P. Lu, R. T. K. Kwok, F. Mahtab, H. S. Kwok, B. Z. Tang, *Chem. Mater.* **2011**, *23*, 2536; J. Huang, X. Yang, J. Wang, C. Zhong, L. Wang, J. Qin, Z. Li, *J. Mater. Chem.* **2012**, *22*, 2478.
- [7] a) S. Kamino, Y. Horio, S. Komeda, K. Minoura, H. Ichikawa, J. Horigome, A. Tatsumi, S. Kaji, T. Yamaguchi, Y. Usami, S. Hirota, S. Enomoto, Y. Fujita, *Chem. Commun.* **2010**, 46, 9013; b) M. Nakamura, T. Sanji, M. Tanaka, *Chem. Eur. J.* **2011**, *17*, 5344; c) T. Hirose, K. Higashiguchi, K. Matsuda, *Chem. Asian J.* **2011**, *6*, 1057; d) K. Kokado, Y. Chujo, *J. Org. Chem.* **2011**, *76*, 316; e) R. Yoshii, A. Nagai, K. Tanaka, Y. Chujo, *Chem. Eur. J.* **2013**, *19*, 4506.
- [8] a) Y. Dong, J. W. Y. Lam, A. Qin, J. Liu, Z. Li, B. Z. Tang, J. Sun, H. S. Kwok, *Appl. Phys. Lett.* **2007**, *91*, 011111; b) A. Qin, C. K. W. Jim, Y. Tang, J. W. Y. Lam, J. Liu, F. Mahtab, P. Gao, B. Z. Tang, *J. Phys. Chem. B* **2008**, *112*, 9281.
- [9] For example, the synthetic procedure of tetraphenylsilole is in accordance with the following paper cited in ref. [4]; E. Braye, W. Hubel, I. Caplier, *J. Am. Chem. Soc.* **1961**, *83*, 4406.
- [10] H.-C. Yeh, W.-C. Wu, C.-T. Chen, *Chem. Commun.* **2003**, 404.
- [11] a) K. Onimura, M. Matsushima, K. Yamabuki, T. Oishi, *Polym. J.* **2010**, *42*, 290; b) M. Nakamura, K. Yamabuki, T. Oishi, K. Onimura, *J. Polym. Sci. Part A J. Polym. Sci. Part A: Polym. Chem.* **2013**, *51*, 4945.
- [12] T. Kato, K. Naka, *Chem. Lett.* **2012**, *41*, 1445.
- [13] K. Kizaki, H. Imoto, T. Kato, K. Naka, *Tetrahedron* **2015**, *71*, 643.
- [14] Q. Qi, J. Zhang, B. Xu, B. Li, S. X.-A. Zhang, W. Tian, *J. Phys. Chem. C* **2013**, *117*, 24997.
- [15] a) Z. Zheng, Z. Yu, M. Yang, F. Jin, Q. Zhang, H. Zhou, J. Wu, Y. Tian, *J. Org. Chem.* **2013**, *78*, 3222; b) H. Unesaki, T. Kato, S. Watase, K. Matsukawa, K. Naka, *Inorg. Chem.* **2014**, *53*, 8270.
- [16] a) Z. Chi, X. Zhang, B. Xu, X. Zhou, C. Ma, Y. Zhang, S. Liu, J. Xu, *Chem. Soc. Rev.* **2012**, *41*, 3878; b) X. Zhang, Z. Chi, Y. Zhang, S. Liu, J. Xu, *J. Mater. Chem. C* **2013**, *1*, 3376.
- [17] N. Miyaura, S. Suzuki, *J. Chem. Soc. Chem. Commun.* **1979**, 866.
- [18] K. Onimura, M. Matsushima, M. Nakamura, T. Tominaga, K. Yamabuki, T. Oishi, *J. Polym. Sci. Part A J. Polym. Sci. Part A: Polym. Chem.* **2011**, *49*, 3550.
- [19] M. P. Robin, P. Wilson, A. B. Mabire, J. K. Kiviahio, J. E. Raymond, D. M. Haddleton, R. K. O'Reilly, *J. Am. Chem. Soc.* **2013**, *135*, 2875.
- [20] W. H. Watson, G. Wu, M. G. Richmond, *J. Chem. Crystallogr.* **2003**, *33*, 983.
- [21] Compounds **3–5** did not have enough solubility to perform ^{13}C NMR analysis. For details, see Experimental Section and Supporting Information.
- [22] The term “*N*-substituent” is used in the sense of “substituent on the N atom of the maleimide ring” for the sake of simplicity.
- [23] Detailed crystal data are listed in Tables S1 and S2 in the Supporting Information. CCDC 1058130 (**7b**) and 1058131 (**7c**) contain the supple-

mentary crystallographic data for this paper. These data can be obtained free of charge from The Cambridge Crystallographic Data Centre via www.ccdc.cam.ac.uk/data_request/cif.

- [24] The term "S-substituted benzene ring" is used in a sense of "benzene ring attached to the maleimide ring through a sulfide bond" for the sake of simplicity.
- [25] *PROCESS-AUTO, RAXIS data-processing software*; Rigaku Corporation: Tokyo, Japan, **1996**.
- [26] T. Higashi, *FS ABSCOR, Program for Absorption Correction*; Rigaku Corporation: Tokyo, Japan, **1995**.
- [27] A. C. Larson in *Crystallographic Computing* (Ed.: F. R. Ahmed), Munksgaard, Copenhagen, **1970**, pp. 291–294.
- [28] P. T. Beurskens, G. Admiraal, G. Beurskens, W. P. Bosman, R. de Gelder, R. Israel, J. M. M. Smits, *The DIRDIF-99 Program System*; Technical Report of the Crystallography Laboratory, University of Nijmegen: Nijmegen, The Netherlands, **1999**.
- [29] P. T. Beurskens, G. Admiraal, G. Beurskens, W. P. Bosman, S. Garcia-Granda, R. O. Gould, J. M. M. Smits, C. Smykalla, *PATY, The DIRDIF Program System*; Technical Report of the Crystallography Laboratory, University of Nijmegen: Nijmegen, The Netherlands, **1992**.
- [30] *CrystalStructure 3.8: Crystal Structure Analysis Package*; Rigaku Americas: The Woodlands, TX, **2000**.
- [31] J. R. Carruthers, J. S. Rollett, P. W. Betteridge, D. Kinna, L. Pearce, A. Larsen, E. Gabe, *CRYSTALS Issue 11*; Chemical Crystallography Laboratory: Oxford, UK, **1999**.

Received: April 19, 2015

Published online on July 14, 2015